MSUCL-173
June 1975

High Resolution Position-Sensitive Proportional Counter*

R.G. Markham and R.G.H. Robertson

Cyclotron Laboratory
Michigan State University, East Lansing, Mi. 48824

ABSTRACT

A counter giving high resolution for lightly ionizing particles incident at 45° has been designed and placed in routine operation in an Enge split-pole magnetic spectrograph. Use of a lumped-constant delay line and inclined cathode pickup stripes results in a very compact unit with high transmission; the collection and readout geometry results in virtual elimination of straggling (energy-loss fluctuations) as a source of resolution degradation. Spectra with total line widths less than 0.25 mm FWHM have been observed with 35 MeV protons.

*Supported by the U.S. National Science Foundation.

I. Introduction

There has been no completely satisfactory detector for use in the focal plane of the popular Enge split-pole spectrograph. Line widths less than 50 μm FWHM have been obtained[1] in this spectrograph far in excess of the capabilities of most detection systems except for nulcear emulsions. The most widely used active detector is perhaps the resistive-anode proportional counter[2,3,4] using either charge division or rise-time effects to locate the event. Although these detectors generally do not give submillimeter resolution, they are preferred because of their low cost, simplicity and ability to transmit the detected particles to backing detectors which serve to reduce background events and to improve the particle identification. Significantly better resolution has been obtained in detectors where the position is determined by relative timing of signals at the ends of a helically wound delay line which serves as the cathode of a proportional counter.[5] This device has good position resolution but is difficult to back with a second detector and is very bulky. A general feature of both types of counters is the steady deterioration of resolution as one goes to higher energy, lighter ions.

Thus, it has been our objective to design a counter which provides high resolution even for lightly ionizing particles, while retaining the virtues of the resistive anode devices. In section 2, we discuss some of the processes taking place in the detection and localization of a particle in a proportional counter. In later sections the design and performance of a

detector which meets the desired objective will be described and theoretical limits for the position resolution will be presented and compared with the results obtained.

2. Position Resolution

2.1 Effects of Energy-loss Fluctuations

The resistive anode counters[2] are capable of position resolution better than 0.3 mm for highly ionizing or normal incident particles; but in use where these conditions are not present, the resolution is generally worse than 1 mm. We feel that the explanation for this effect is that energy loss fluctuations can lead to position fluctuations for non-normal particles. In an early work, Miller et al.[4] made an estimate of the seriousness of this effect based on the Bohr formula for the variance of the energy loss distribution. It seems these calculations are in error and underestimate the severity of the problem. Braid, Ford and Stoltzfus[6] have since performed a Monte-Carlo calculation with a Vavilov[7] distirbution of energy loss, which is far more valid for particles with energies of interest.

We also have calculated the energy-loss fluctuation effects by integration of the Vavilov distributions for energy loss in the halves of the counter. We assume that the detected position is the center of gravity of the energy loss and is given by

$$X = \frac{E_1X_1 - E_2X_2}{E_1 + E_2} \qquad (1)$$

where $E_{1(2)}$ and $X_{1(2)}$ are the energy loss and its center of gravity for the first (second) half of the counter. It is assumed that X_1 and X_2 correspond to the geometrical centers of the

particle trajectory in the first and second halves of the counter. The probability that X will have a particular value is then

$$P(X) \propto \int_0^\infty P_1(E_1)P_2(E_2)dE_1 \qquad (2)$$

where equation 1 is used to solve for E_2 in terms of E_1 and X, and P(E) is the Vavilov energy loss distribution. The integral is then done for a range of values of X to produce the line shape and deduce its width ΔX_o.

To account for variations in the centroids X_1 and X_2, we proceed to subdivide the two halves of the counter and calculate the variation $\Delta X_{1(2)}$ we expect to get for $X_{1(2)}$. These are then added in quadrature to the variations ΔX_o for fixed $X_{1(2)}$.

$$\Delta X = \sqrt{\Delta X_o^2 + \left(\frac{E_1\Delta X_1}{E_1+E_2}\right)^2 + \left(\frac{E_2\Delta X_2}{E_1+E_2}\right)^2}$$

$$\Delta X \approx \sqrt{\Delta X_o^2 + 1/2\ \Delta X_{1(2)}^2}$$

For the Landau and Gaussian limits of the Vavilov distribution, this amounts to a 7 to 15% correction. Thus, higher order corrections are not required.

The results of these calculations are shown in Fig. 1 for a 1.5 cm deep counter filled with 1 atmosphere of 88% He + 9% He + 5% CO_2. For line widths below about ∿1.6 mm the curves scale roughly as $\sqrt{D/P}$ where D is the depth of the counter and P is the gas pressure. Above ∿1.6 mm the curves flatten and become essentially pressure independent and scale as D. The slight decrease at high energies is probably artificial as the Vavilov theory is no longer valid for such lightly ionizing particles. Since the

maximum value for the line width is the same for all particle types and is proportional D, we find that a counter 2 mm thick will give a limiting resolution of ∿0.3 mm FWHM; and in fact, all but the most highly ionizing particles will be at this limit.

It is our contention that, for moderate and low ionizing particles incident at 45° to the normal, the resolution of both resistive anode and helix counters is dominated by energy-loss fluctuation effects. The sole difference is that the time derivation methods used in the helix counter make that device effectively very thin because the electron drift time discriminates against ionization occurring far from the wire. The effective depth depends not only on the time derivation technique and its operating parameters, but also on the anode geometry, the vertical position of the track and the gas properties (particularly electron and positive ion drift velocities). According to our calculations, an effective thickness of ∿2 mm would give line widths consistent with reported values for helix counters.[5] A further reduction in the effect of energy-loss fluctuations can be expected when appreciable saturation of the gas gain is present, as this tends to smooth out the variations in collected charge along the projected path. A gas which has this property is the "magic" gas mixture containing Freon.[8]

2.2 Energy Loss Straggling Compensation

In order to make energy-loss fluctuation effects unimportant, each primary ionization event along a particle trajectory should result in the same computed position. (This is in contrast with

the usual method where, except for normally incident particles, the computed position is an average of many different contributions from ion pairs created along the particle's trajectory.) To implement this, the counter volume is effectively subdivided into five thinner volumes by replacing the single anode wire with five wires at a 2mm spacing in the plane of the particle trajectory (Figs. 2 and 3). The electric field is desired to be normal to the wire plane everywhere (except close to the wires). The correct field shape in the active region is achieved by adding four more wires, two at the front and two at the back of the plane. These guard wires have a much larger diameter to prevent multiplication from occuring on them--thus they absorb without amplification any electrons produced outside the desired active region. As a result of this geometry, ionization originating anywhere in the active volume produces multiplication only on the wire directly above (or below), and nowhere else. Underneath the anode plane is a cathode plane comprised of metallic stripes oriented parallel to the particle trajectory, (i.e. at 45° to the normal). (The correct angle is actually slightly greater due to fringe field effects, as will be discussed.) The charge induced on the cathode by avalanches forming near each anode wire as a particle passes through the counter is thus always in the same location relative to the cathode stripes. Energy loss variations from wire to wire therefore do not lead to position variations.

Translation of the induced cathode charge to a position signal is accomplished by connecting each cathode stripe to a tap

on a commercial delay line following the method of Beardsworth et al.[9] and measuring the propagation time to the ends of the delay line.

Energy loss fluctuations within the collection region of each wire lead to centroid fluctuations at each multiplication site. The result is that the contribution to the overall line width arising from energy loss straggling alone with this counter design will be $1/\sqrt{5}$ times the line width of a counter with thickness equal to the anode wire spacing. For gases at atmospheric pressure and below, and an anode wire spacing of 2 mm, the straggling contribution is calculated to be about 0.13 mm FWHM.

A further advantage of the design is that it lends itself very naturally to the addition of backing counters. Its transparency is high--only the anode plane obstructs the passage of ions.

3. Design of Counter

3.1 Anode Design

In the discussion of Sec. 2.2 it was assumed that all electrons went to the nearest anode wire and that the multiplication was the same on each active wire and zero on the guard wires. By tests and conductive paper studies it was concluded that two guard wires at the front and back were the minimum one could use. With only one, the outermost active wires have higher electric fields at their surface with weaker fields further away.

The guard wires were chosen to have a large enough radius to insure no multiplication when biased at the appropriate voltage to give them the same charge per unit length as the active wires.

The semi-empirical equation of Wolff[10] for the gas amplification as a function of bias voltage and gas pressure was used to select the guard wire diameter. This was accomplished by expressing the equation in terms of the charge per unit length q on the wire and the diameter d. Then one obtains for the amplification

$$A = \left(\frac{4q'}{Kpd}\right)^{2q'\frac{\ln 2}{\Delta V}} \qquad q' = \frac{q}{4\pi\varepsilon_o} \text{ (Volts)}$$

where P is the gas pressure and K and ΔV are empirical constants. The charge per unit length was computed for an infinite array of uniformly spaced, small diameter wires between two conducting planes. For standard operating conditions it was found that A would be less than unity for $d = 12.7 \times 10^{-3}$ cm. In practice, the gain on the outermost guard wires is larger because of their proximity to nearby grounded surfaces. However, experimental tests were made in which each wire of the plane was illuminated independently with α-particles passing normally through the plane. These tests showed that the guard wires had a gain at least an order of magnitude lower than the central wires, and that the ratio of bias voltages for the guard wires and central wires was given correctly by the prescription above.

3.2 Effects of Discretization of the Cathode Plane

Although a relatively coarse spacing of the cathode pickup stripes, 2.54 mm, is used, it is nevertheless possible to achieve very high resolution of the position of the induced charge signals because of an interpolation property. The induced charge covers a distance comparable to the anode-cathode spacing, and the time centroids of pulses arriving at the ends of the delay line still

contain high precision position information. (Sufficient integration is therefore essential to insure that time derivation techniques do yield the centroid of the charge distribution. Qualitatively, integration times should be substantially longer than the time difference between adjacent stripes (10 ns in the present design).

The principal effect of discretization of the cathode plane is periodic differential non-linearity. The wavelength is equal to the stripe spacing, and the amplitude may readily be estimated. Lee, Sobottka and Thiessen[11] have derived an expression for the spatial distribution of induced charge in a geometry similar to ours. (Note, however, that this distribution is somewhat controversial.[12]) In their notation, the induced charge on the cathode is proportional to $[1 + \cosh \frac{\pi z}{b}]^{-1}$ where "b" is the anode-cathode spacing, and "z" the distance parallel to the anode wires from a point charge located very near the anode wires. Thus the charge induced on the cathode between z_1 and z_2 is proportional to $(\arctan e^{\zeta 2/2} - \arctan e^{\zeta 1/2})$ where $\zeta = z/b$, and the centroid of the time distribution will correspond to the position given by

$$C = \sum_i 1/2(Z_{i+1} + Z_i)[\arctan (e^{\zeta i+1/2}) - \arctan (e^{\zeta i/2})]$$

Evaluating this expression numerically for various positions of the charge relative to the cathode stripes, we found, for the geometry in use (anode-cathode spacing 5 mm, stripe spacing 2.54 mm) a maximum deviation from linearity of approximately 5 μm. This effect will thus be unimportant for all but the most precise work, and is, furthermore, insignificant compared to the contribution of variations in delay-time from tap-to-tap on the delay line.

3.3 Delay Line

The delay line used is a lumped constant design provided by Data Delay Devices, Inc.[13] Its electrical and physical properties are summarized in Table 1. Besides being very compact, the line also has the highly desirable property that it is free of dispersion. The variation of delay with frequency was measured to be less than ±1% for frequencies between 250 kHz and 10 MHZ. The effect of the line on pulse shape is similar to that of an R-C-integrator having a time constant of 35 nsec for pulses going the full length of the line.

There is a fairly large variation in the delay per tap in this line which can be a source of differential non-linearity. Fortunately the charge from each event is distributed over several taps so that random variations tend to be averaged out; large scale systematic variations can be removed by careful calibration techniques. The tap-to-tap delay variations are due to the difficulty of maintaining rigorous specifications on components having small values of inductance and capacitance. It is our understanding that this problem would be less severe for lines of lower impedance and higher delay per tap.

Noise considerations suggest that one should use a high impedance line; but the above considerations support the use of a low impedance line. The optimal solution will then depend on the type of particle being detected (signal to noise) and the amount of differential non-linearity tolerable. Since noise is not a serious problem for 35 MeV protons (see Section 5.0), a lower impedance line would seem to be recommended especially for applications involving more heavily ionizing particles.

However, very promising characteristics have been measured for a new continuously wound distributed line.[13] Not only is its impedance higher (800 Ω), but its differential non-linearity is extremely low.

3.4 Counter Construction

The counter consists of three major parts: the body, the anode bridge, and the delay-line and pickup-stripe assembly. The counter body is machined from a single piece of stress-relieved aluminum. Its over-all dimensions are approximately 5 cm x 41 cm x 5.4 cm deep. The active length is 25 cm, leaving enough space at each end to accommodate the anode wire supports and biasing resistors. Additional length is also required to allow all entering particles (at 45°) to pass through the counter. A cross section and photograph of the assembled counter, without the front window, can be seen in Fig. 2 and 4. The front half of the body has been machined out extensively to make room for the removable anode bridge and delay line. The back half forms a conventional center-wire proportional counter for accurate energy-loss measurement. The sturdy one-piece construction limits the vertical expansion at the middle to about 0.5 mm for 1 atmosphere differential pressure. Much of this strain is not transmitted to the anode or delay-line structures because they are attached by two bolts each to the thicker back section of the counter.

To facilitate mounting the anode wires, a removable bridge was made, consisting of a solid aluminum bar with plastic terminal blocks on each end. The ends of the wires are held under machine

screws and the spacing is maintained at 1.9 mm by stretching the wires across exposed threads of nylon screws mounted in the terminal blocks. The thread pitch determines the possible wire spacings. The active wires are 25 μm tungsten and the guard wires are 127 μm copper.

The delay line and pickup stripes form another removable unit. The pickup stripe board is an etched circuit board bonded to an aluminum frame. The stripes are soldered to the delay line taps at the back of the board with the delay line being suspended underneath by its 100 taps. This entire unit is only 1.1 cm tall and 3.8 cm deep. When assembled the back edge of the board extends into the second proportional counter volume and so must be shielded from the single wire. A grounded, aluminized Mylar foil covering the affected part of the stripes provides adequate shielding.

The active volumes of the front and back counters are separated by a metal foil--2.5 μm-Havar[14]-fastened along three sides to a brass frame. This frame is held in place by the mounting bolts for the anode bridge.

Standard BNC and SHV cable fittings were used for the delay line signals and high voltage power. The SHV fittings were made gas-tight by applying red enamel to the center pin-insulator interface. These fittings have proven to be both leak-free and able to withstand the high operating voltages. Gas line connections were made at each end to allow continuous gas flow during operation.

4. Operation and Performance

4.1 Operation

The gas used in the counter is normally pure propane at one third atmospheric pressure. Propane gives reproducible, high gain and freedom from sparking at pressures low enough that small-angle scattering in the gas is a negligible contribution to the resolution. The gas is flowed continuously and the pressure is regulated by a Cartesian manostat. The multiplying wires are biased at about 3200 V, with the guard wires maintained at 87% of that value by a resistance divider chain inside the counter.

It is desirable to connect the anode wires to a low-impedance termination so that pulses are not induced on the cathode by the negative excursions of the anode (a condition which leads to poor resolution near the ends of the counter). However, if the anode termination has a high stored charge, there is a risk of destroying the delay line in the event of a spark. To circumvent this, the anodes are biased through a fast-recovery, 10-kV diode, Sarkes-Tarzian type 20 AFR100 as shown in Fig. 5. The small stored charge of this diode is sufficient to maintain bias for normal pulses, but the diode decouples the anode from the 120 pf capacitor during a spark. In this way the peak voltage on the delay line is limited to approximately 300 V. A DC path to ground is provided by 10 kΩ resistors at the ends of the delay line.

"Electronically cooled" preamplifiers[15] are used. The preamplifiers are charge sensitive but have an input impedance that is resistive with a magnitude of 500 ohms to match the

delay line impedance. They were modified from the schematic shown in Fig. 8 of ref. 15 by the addition of a 10 Ω resistor in the emitter circuity of the input transitors. This modification did not seem to alter the performance appreciably but does make the input transistors less prone to damage from transients.

The preamplifier signals are processed by RC-CR shaping amplifiers--Ortec model 454-with τ_{int}=50 nsec and $\tau_{dif.}$=100 nsec. The shaped signals are fed to constant fraction discriminators--Ortec model 473-which are operated in the amplitude and rise-time compensated mode with 60 nsec delay cables. The discriminators were modified to make the optional 1 usec enforced dead time apply when external delay cables are used. It is necessary to delay the output of one of the discriminators 1 usec to ensure that it always reaches the stop input of the TAC after the start signal. A variable delay can be used for this purpose, but it must be of exceptionally high quality. We have used the Ortec model 416A gate and delay generator successfully, but it is marginal over long periods since delay changes of one part in 10^4 are easily detected when doing high resolution work.

The second proportional counter signal is processed by conventional electronics with a single channel analyser used to select a limited range of ΔE signals. The counter is usually backed further by a scintillator and photomultiplier which give characteristic pulse height and time-of-flight referred to the cyclotron.[16] These signals are processed by single-channel analysers whose outputs, if they satisfy a coincidence requirement, strobe the position TAC and ΔE linear-gate-and-stretcher

outputs. The strobing places these signals (and others from the backing scintillator) in time-coincidence for multiparameter computer processing.

4.2 Operational Experimence

The counter has been used by various members of the laboratory in (p,p'), (p,t), (p,^{3}He) (p,α) (α,d), (^{3}He,p) and (^{3}He,d) experiments. Because accurate dispersion matching is obtained most easily for (p,p) reactions, these experiments have had the best resolution by far. A typical spectrum obtained in a ^{40,44,48}Ca(p,p) experiment[17] on a mixed isotope target at 30.3 MeV is shown in Fig. 6. The peak widths (0.26 to 0.28 mm FWHM) were extracted by calculating the rms widths and assuming Gaussian line shapes. The contribution due to the beam was not determined in this case but is presumed to be small. Figures 7 and 8 show spectra obtained in ^{52}Cr(p,α)^{49}V and ^{15}N(^{3}He,d)^{16}O experiments.[18,19] In both cases the resolution was beam and target limited. The notable feature of these spectra is the lack of background. The peak-to-background ratio in the (^{3}He,d) spectrum exceeds 10^4. This was achieved by redundant identification of the detected particles on the basis of energy loss, time-of-flight and stopping energy. The scintillator placed behind the counter was used to derive the time and energy information. The least ionizing particle detected with the counter has been 70 MeV protons from a ^{12}C(^{3}He,p)^{14}N experiment. The resolution was 0.5 mm FWHM, consistent with the beam resolution determined by elastic scattering of ^{3}He.

Although no detialed tests of the performance of the counter at high count rates have been made, good spectra have been taken at average rates of 25 kHz.

4.3 Contributiions to the line width

In Section 2 the effect of energy loss fluctuations on position determination was discussed in some detail. For the present counter two contributions to the line width can be distinguished, the first being due to the energy loss fluctuations within the active volume of each wire and the second arising from not having the pickup stripes at exactly the proper angle. The first effect can be estimated as $1/\sqrt{5}$ times the effect for one 2 mm thick counter. For the gas filling we use, propane at one third atmosphere, it is calculated to be less than 0.13 mm.

As mentioned earlier the second effect can be completely removed by placing the stripes at the correct angle. Intuitively, the correct angle should be 45° for 45° incident particles and this is how the counter used in the present measurements was constructed. However, the pickup stripes receive only a fraction of the total induced charge (they are of finite length) and as a result the centroid of the induced charge distribution on the stripes from the avalanche on a single wire does not lie directly below the avalanche on that wire. How this effect arises can be understood from Fig. 9 which illustrates the case of a point charge above an infinite conducting plane. The induced charge is distributed symmetrically about the point on the plane directly below the point charge and so the centroid of the distribution is directly below the charge. But if one computes the centroid for only that part of the plane between the dashed lines, corresponding to the actual extent of the cathode surface, one finds that the centroid near the edges is shifted inwards. Applying this idea to the actual counter we

should expect that for 45° stripes best resolution should be obtained for particles incident at somewhat less than 45° to the normal. Indeed, the loci of the induced charge centroids will not in general be straight lines. However, accurate calculation of the loci appears to be impractical, and the best approach seems to be to derive an optimum angle for straight stripes from plots such as Fig. 10, which shows results of a measurement of the resolution as a function of incident angle. This was done by bringing 35 MeV elastic protons to focus on the counter and then rotating the counter about the point of focus. The optimum angle is clearly displaced by about three degrees in the direction expected. The contribution to the line width at 45° incidence is about 0.1 mm. Figure 11 shows the measured spectrum observed at the optimum angle of incidence. The overall resolution is 0.24 mm FWHM.

Multiple scattering in the entrance window and counter gas can be a serious problem, especially for more heavily ionizing particles. The entrance foil currently in use is 6 μm thick aluminized Mylar although 13 μm Kapton was used in the above measurements. For the 35 MeV proton detected it is estimated that window scattering made a 70 μm contribution to the line width. (The low gas pressure used would permit a substantially thinner window.) Scattering in the gas can be very severe if high-Z gases are used. The problem is largely eliminated by the use of a pure hydrocarbon gas such as propane at a reduced pressure. With our standard filling of one third atmosphere and 35 MeV protons multiple scattering in the gas is only a 50 μm effect; for one atmosphere of P-10 it would be 160 μm. As with

the window scattering, the size of this contribution increases greatly for heavily ionizing particles.

Table 2 summarizes the above contributions. These, together with an actual line width of 100 μm (measured using the "speculator" described by Blosser et al.[20]) add in quadrature to a total of 220 μm FWHM. The total measured line width is 260 μm at 45°. The residual is then due to the several other effects not yet discussed and to the uncertainty in estimating the ones we have.

The remaining effects associated with charge collection and multiplication in the gas are diffusion of the primary electrons during migration to the anode wires, variations (and fluctuations) of the multiplication along the wires, and erratic spreading of the avalanche. These effects are difficult to estimate or to isolate experimentally. The best approach is to choose a gas with a small ratio of transverse diffusion coefficient to mobility, and with a high opacity for hard UV photons responsible for spreading of the avalanche. We have some evidence that photon-assisted propagation of the avalanche can be very important from our experinece with under-quenched gases. A mixture of 95% He-5% C_3H_8 was tried and it was observed that the counter did not operate stably at high gain due to geiger breakdown and the resolution was worse than one millimeter. There is no evidence for geiger breakdown of propane at one third atmosphere but at sufficiently low pressures it may be expected than any gas will behave poorly since the photon range becomes arbitrarily long.

Another contribution to the residual line widths is timing inaccuracies associated with thermal and induced electronic noise. Detailed consideration of the thermal noise contribution has been described by Radeka,[15] but it appears that, at present, induced noise (principally from the cyclotron r.f. system) accounts for the larger fraction of the elctronic noise. The combined effect of these two noise sources is always small relative to the observed linewidths, but perhaps is responsible for a significant part of the residual.

5. Acknowledgements

We wish to extend our thanks to Dr. S. Iwata and the Brookhaven group for providing us with information on delay lines, to Mr. J. Lupi of Data Delay Devices for his special efforts to produce high quality delay lines, and to Professor J.A. Nolen, Jr. for help in many of the high-resolution measurements.

References

1. J.A. Nolen, Jr. and P.S. Miller, BAPS 19, 1026(1974).
2. H.W. Fulbright, R.G. Markham and W.A. Lanford, Nucl. Instr. and Meth. 108, 125(1973).
3. C.J. Borkowski and M.K. Kopp, Rev. Sci. Instr. 39, 1515 (1968).
4. G.L. Miller, N. Williams, A Senator and R. Stensgaard, Nucl. Instr. and Meth. 91, 389(1971).
5. D.M. Lee, S.E. Sobottka and H.A. Thiessen, Nucl. Instr. and Meth. 109, 421(1973).
6. T.H. Braid, J. Ford and J. Stoltzfus, private communication.
7. P. Vavilov, Zh. Eksp. Theor. Fiz. 32, 920(1957) [JETP 5, 749(1957)].
8. R. Bouclier, G. Charpak, Z. Dimcovski, G. Fischer, F. Sauli, G. Cognet and G. Flugge, Nucl. Instr. and Meth. 88, 149 (1970).
9. E. Beadsworth, J. Fischer, S. Iwata, M.J. LeVine, V. Radeka and C.E. Thorn, to be published in Nucl. Instr. and Meth.
10. R.S. Wolff, Nucl. Instr. and Meth. 115, 461(1974).
11. D.M. Lee, S.E. Sobottka and H.A. Thiessen, Nucl. Instr. and Meth. 104, 179(1972).
12. J.L. Lacy and R.S. Lindsey, Nucl. Instr. and Meth. 119, 483(1974).
13. Data Delay Devices, Inc., 253 Crooks Ave., Clifton, New Jersey 07011.
14. A.D. Mackay, Inc. 198 Broadway, New York 38, New York.
15. V. Radeka, IEEE Trans. Nucl. Sci. NS-21, No. 1, 51(1974).

16. E. Kashy, W. Benenson, I.D. Proctor, P. Hauge and G. Bertsch, Phys. Rev. C7, 2251(1973).
17. Sam M. Austin, E. Kashy, C.H. King, Jr. and R.G. Markham, private communication.
18. J.A. Nolen, Jr and P.A. Smith, private communication.
19. R.G.H. Robertson and Sam M. Austin, private communication.
20. H.G. Blosser, G.M. Crawely, R. DeForest, E. Kashy and B.H. Wildenthal, Nucl. Instr. and Meth. 91, 1(1971).

Table 1: Delay line properties

Impedance	500 ohms (nominal)
3db bandwidth	4.6 MHz
Delay:	
total	1μ sec
variation with frequency	$<\pm$1% 250 kHz to 10 MHz
per tap	10 nsec
variation per tap	$\pm$10% maximum
Tap spacing	2.54 mm (in line)
Packaged size	0.8 x 3.2 x 28 cm

Table 2: Contributions to the observed line width.

Source	FWHM (mm) for 35 MeV Protons	Alphas
Optimum angle not 45°	0.10 mm	0.08
Energy loss fluctuations	0.13	0.10
Multiple scattering, window	0.10	0.24
gas	0.05	0.24
Actual line width	0.10	
Total	0.22	
Observed	0.26	
Residual	0.14	

Figure Captions

Fig. 1--Calculated position uncertainty due to energy loss fluctuations for a counter 1.5 cm deep with 1 atm of 86% Ne + 9% He + 5% CO_2.

Fig. 2--Schematic cross section of the counter. The various parts are: A) window frames, B) anode support, C) separator foil frame, D) anode wires--five active and four guards, E) anode wire for ΔE counter, F) pickup stripe board, G) frame for delay line and board, and H) delay line.

Fig. 3--Schematic (plan view) of counter.

Fig. 4--Photograph of counter with window removed.

Fig. 5--Schematic of high voltage biasing and protection network.

Fig. 6--A spectrum from a $^{40,44,48}Ca(p,p)$ experiment[17] using 30.3 MeV protons on a mixed isotope target. The solid angle was 0.3 ms.

Fig. 7--A spectrum from a $^{52}Cr(p,\alpha)^{49}V$ experiment[18] using 35 MeV protons.

Fig. 8--A spectrum from a $^{15}N(^{3}He,d)^{16}O$ experiment.[19]

Fig. 9--Equal charge density contours are shown for a point charge above an infinite conducting plane. The "X" represents the location of the centroid of the charge between the dashed lines.

Fig. 10--Reduced line width as a function of angle of the particles to the normal. The measured line width was reduced by subtracting in quadrature the smallest measured value. The curve is a prediction based on energy loss fluctuations and the assumption that the optimum angle is 42°.

Fig. 11--The narrowest line from $^{12}C(p,p)^{12}C$ tests recorded at 35 MeV at 20° using a 0.3 ms aperture. The counter was rotated so that the particles were incident at the optimum angle 42° to the normal.

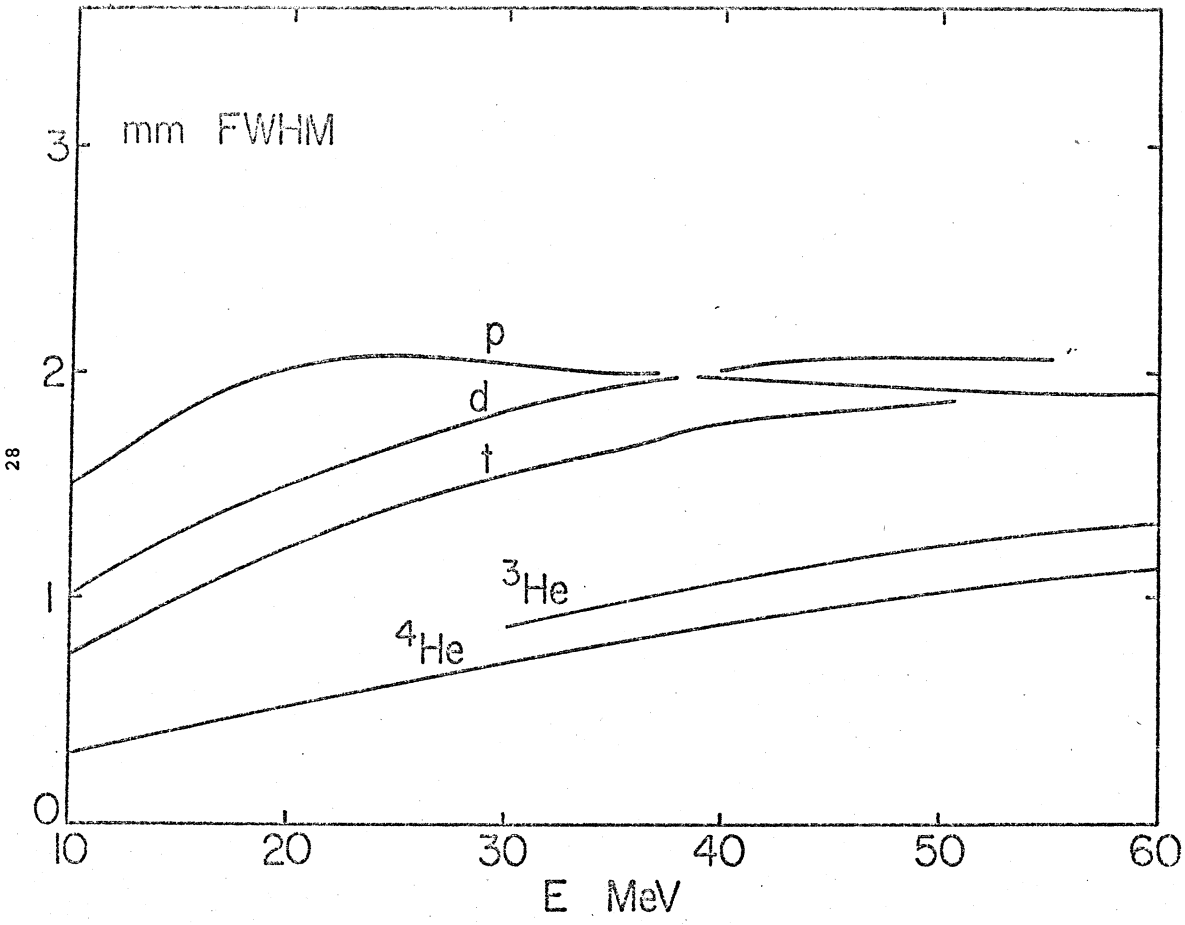

28

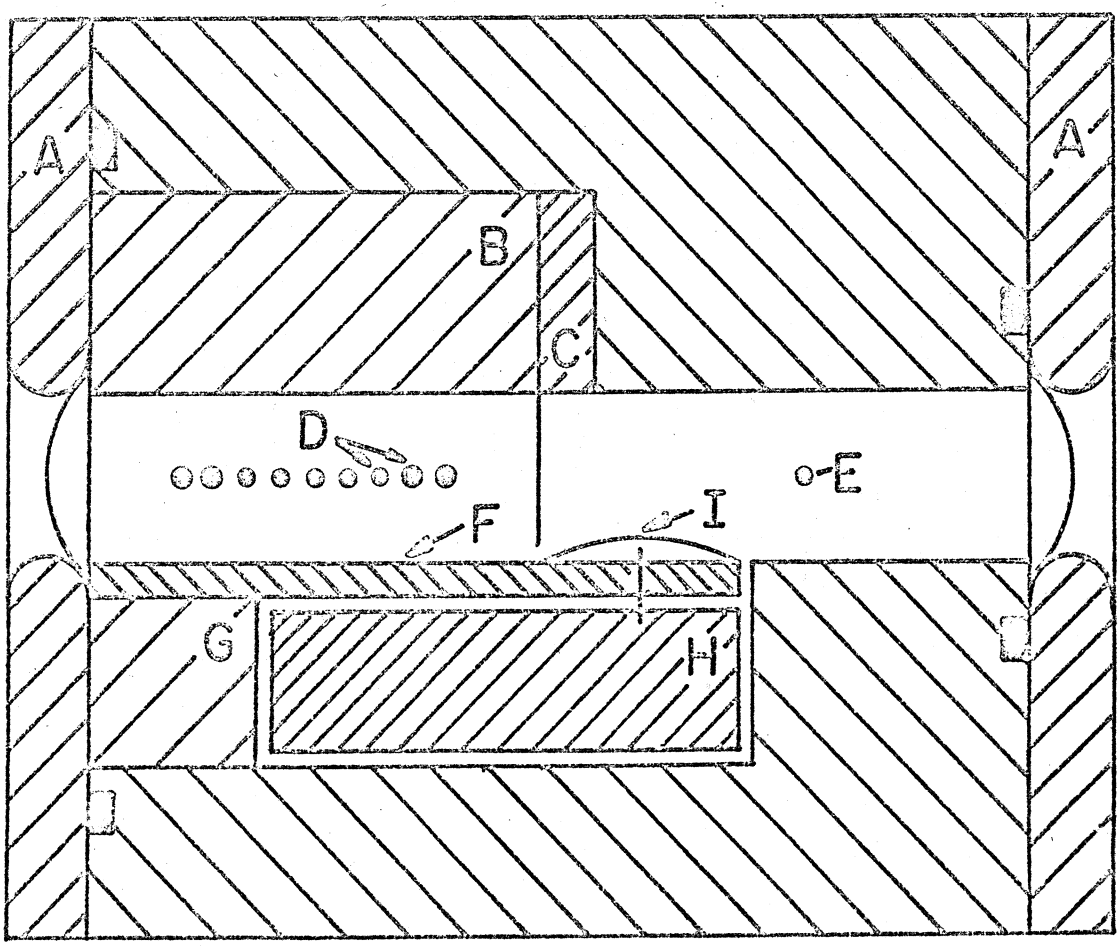

27

30

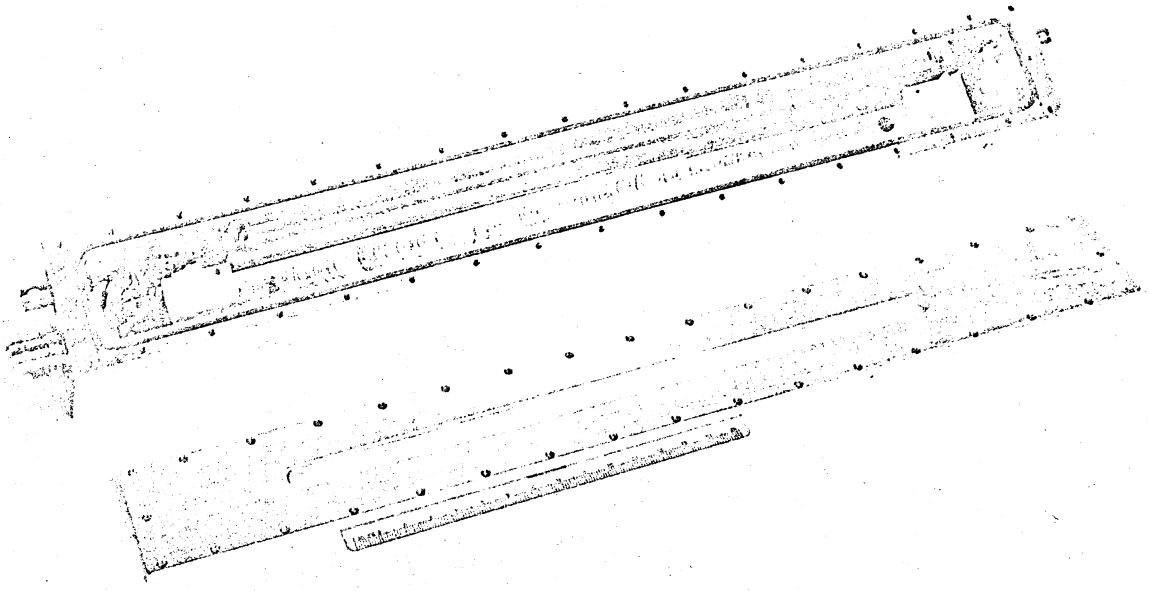

29

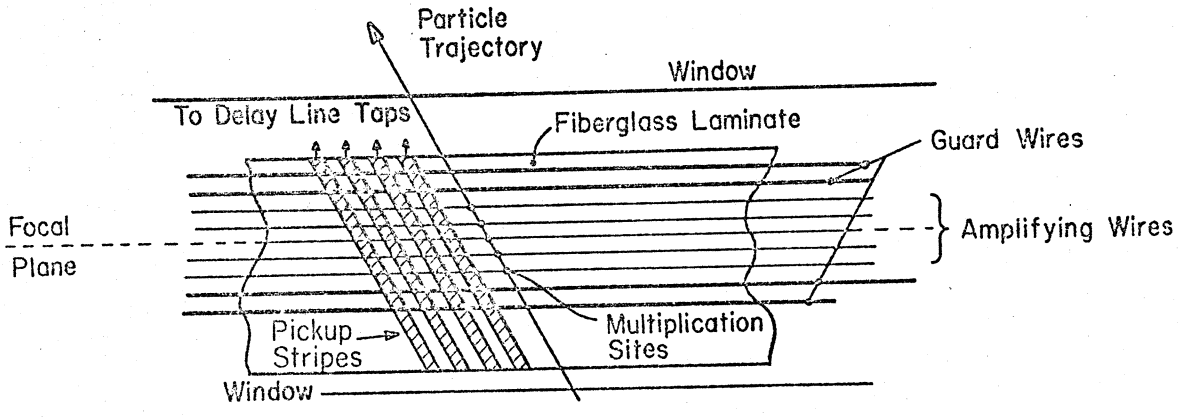

SCHEMATIC (Plan View) OF COUNTER

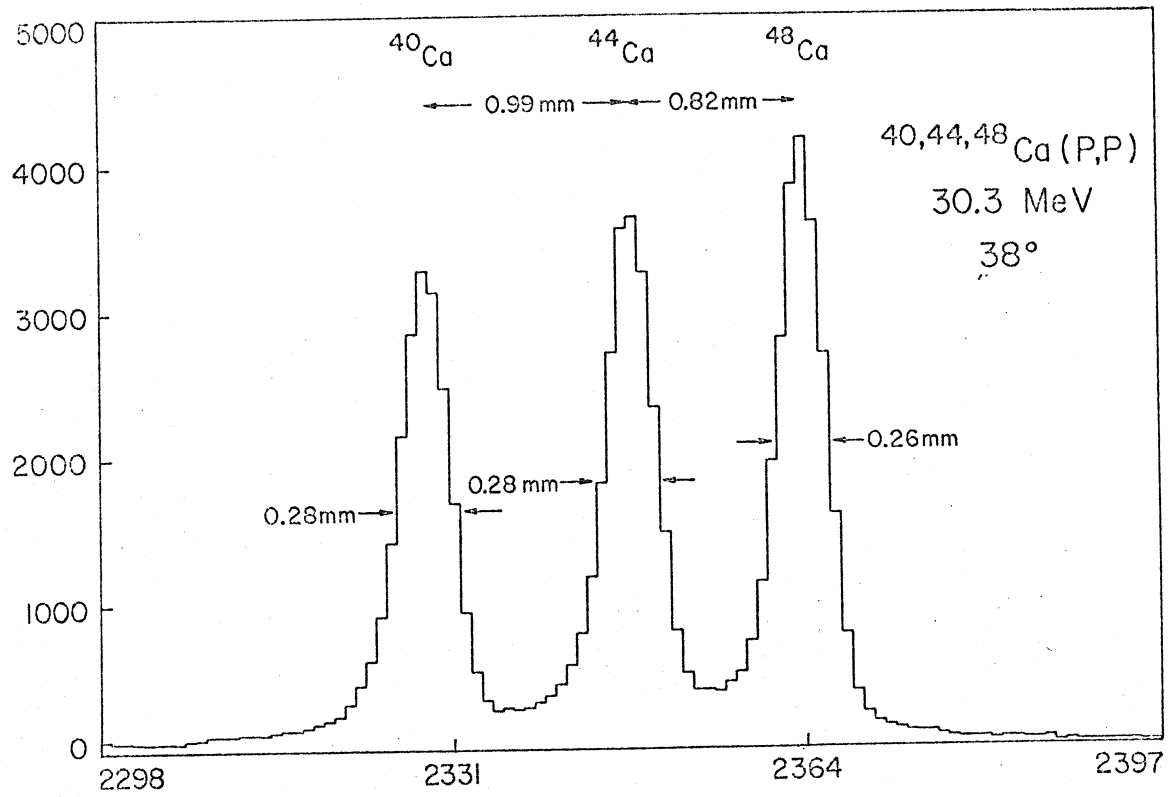
5000
4000
3000
2000
1000
0
^{40}Ca
^{44}Ca
^{48}Ca
0.99 mm
0.82mm
^{40,44,48}Ca (P,P)
30.3 MeV
38°
0.28mm
0.28 mm
0.26mm
2298
2331
2364
2397

32

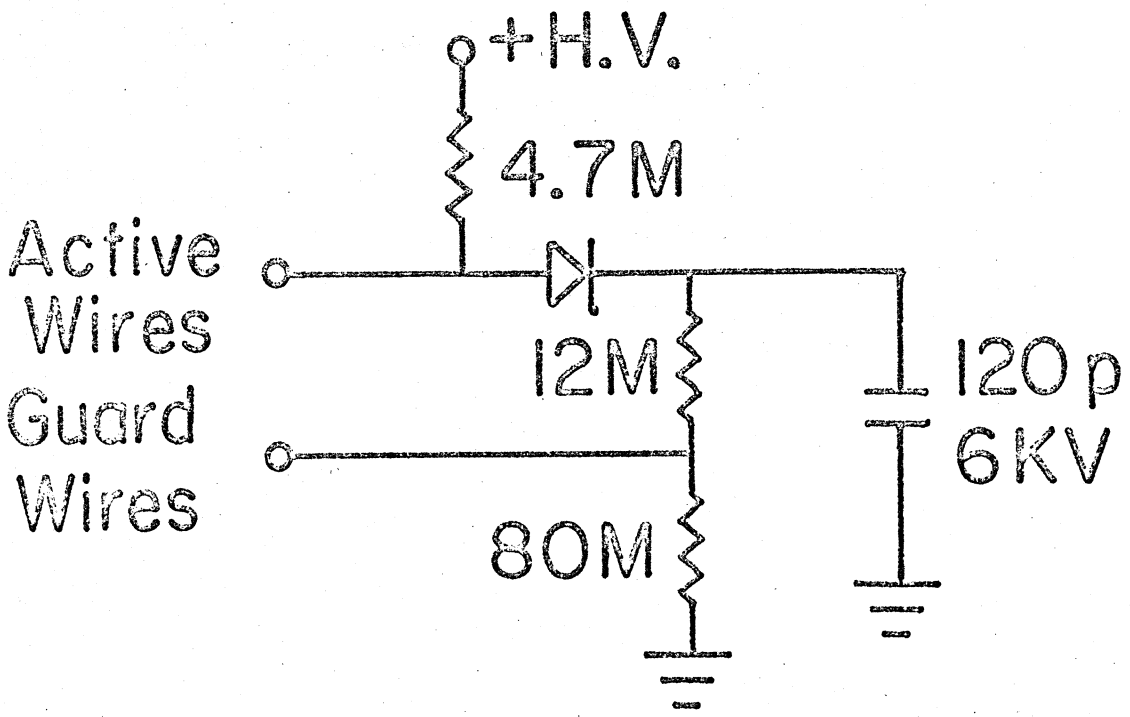
+H.V.
4.7M
Active Wires
Guard Wires
12M
80M
120 p
6KV

31

34

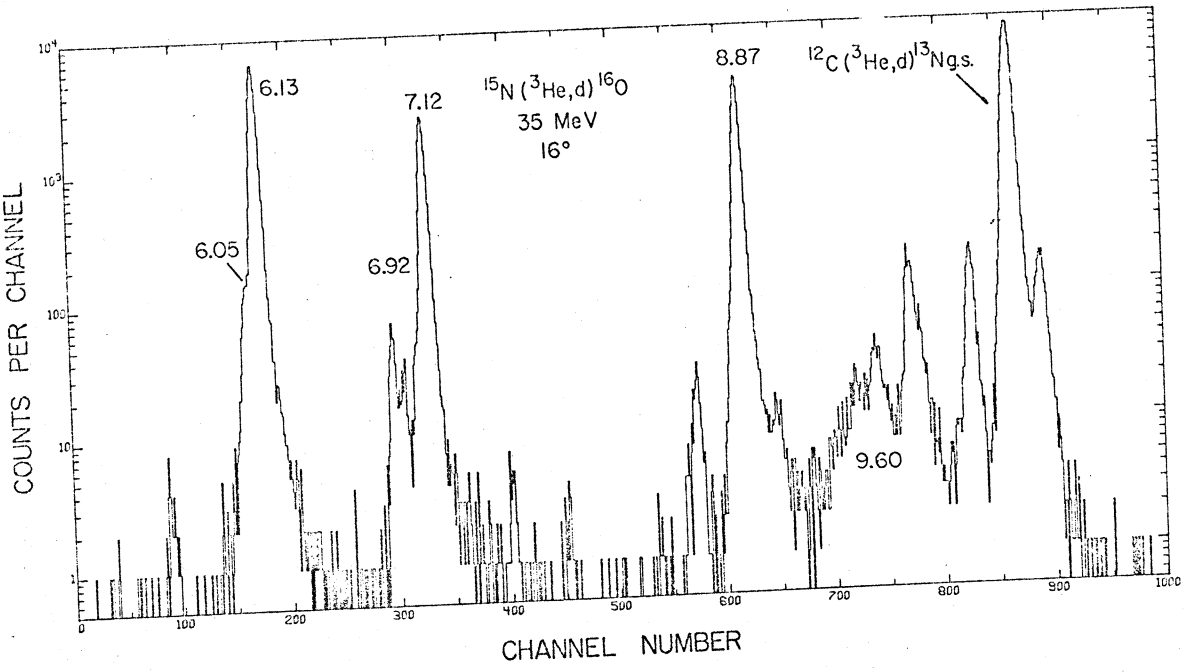
$^{15}N(^3He,d)^{16}O$
35 MeV
16°
6.13
7.12
8.87
$^{12}C(^3He,d)^{13}N$ g.s.
6.05
6.92
9.60
COUNTS PER CHANNEL
CHANNEL NUMBER

33

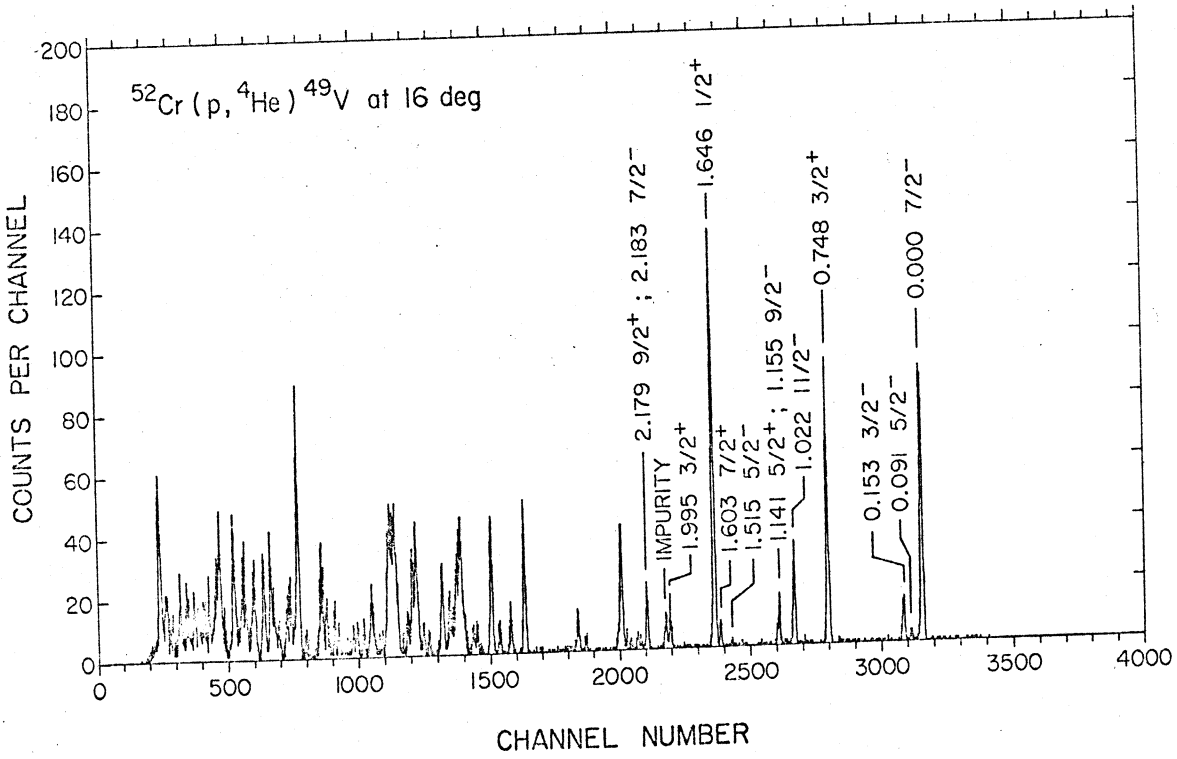
$^{52}Cr(p,^4He)^{49}V$ at 16 deg
2.179 9/2+ ; 2.183 7/2−
IMPURITY
1.995 3/2+
1.646 1/2+
1.603 7/2+
1.515 5/2−
1.141 5/2+ ; 1.155 9/2−
1.022 11/2−
0.748 3/2+
0.153 3/2−
0.091 5/2−
0.000 7/2−
COUNTS PER CHANNEL
CHANNEL NUMBER

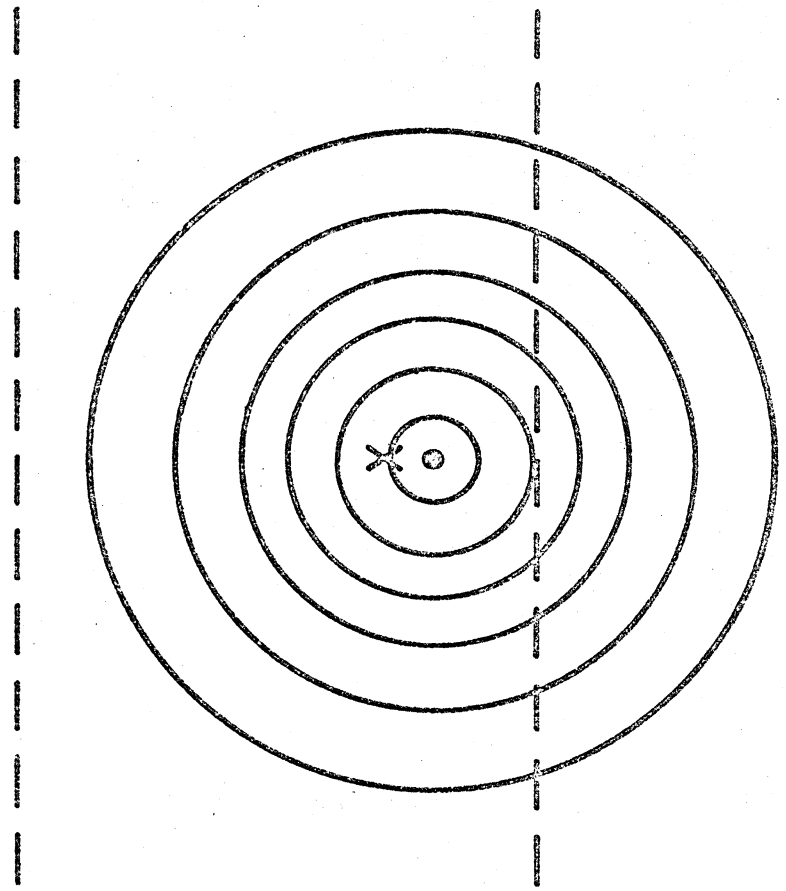

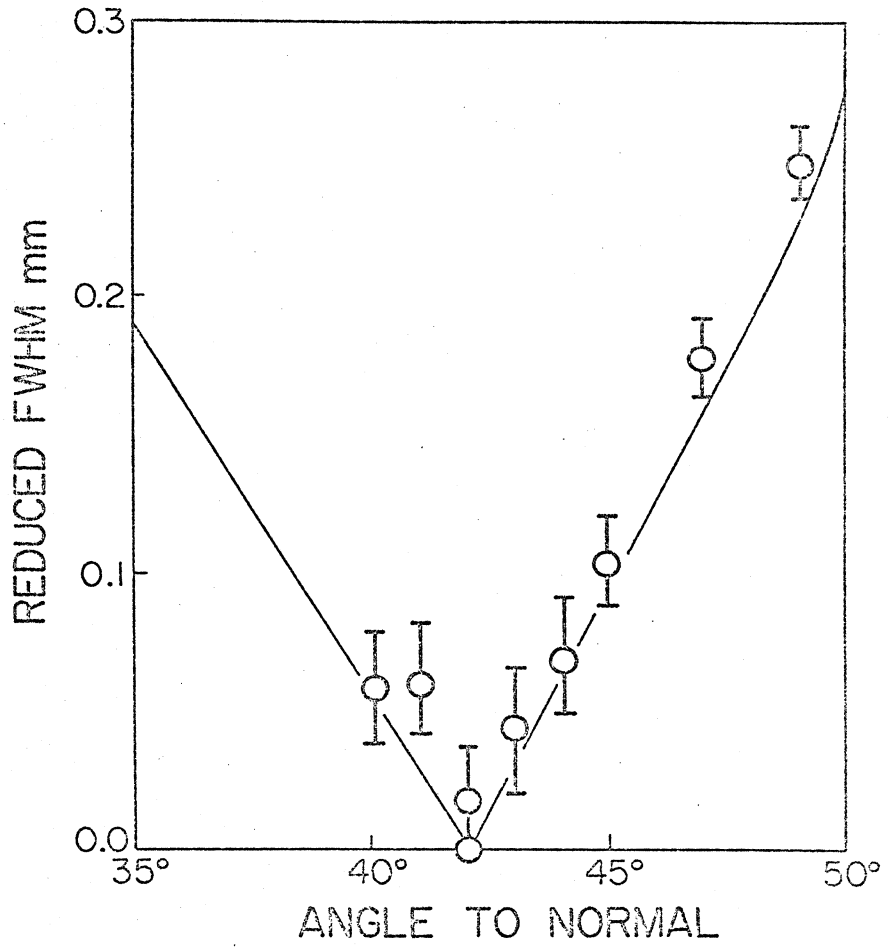
0.3
0.2
0.1
0.0
REDUCED FWHM mm
35°
40°
45°
50°
ANGLE TO NORMAL

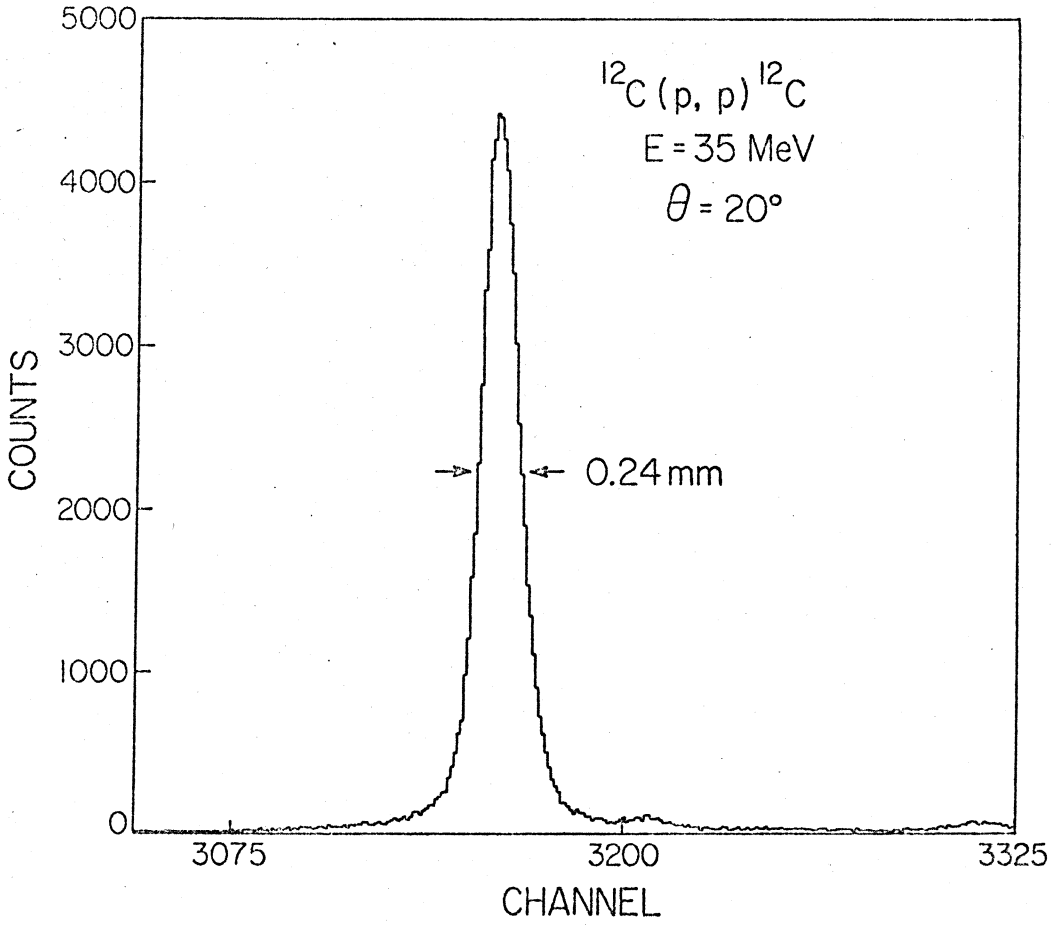
5000
4000
3000
2000
1000
0
COUNTS
$^{12}C(p, p)^{12}C$
E = 35 MeV
θ = 20°
0.24 mm
3075
3200
3325
CHANNEL